Cent. Eur. For. J. 65 (2019) 000–000 sciendo DOI: 10.2478/forj-2019-0020
CENTRAL EUROPEAN Forestry Journal
http://www.nlcsk.sk/fj/

ORIGINAL PAPER

Suitability of MODIS-based NDVI index for forest monitoring and its seasonal applications in Central Europe

Ivan Barka[1]*, Tomáš Bucha[1], Tamás Molnár[2], Norbert Móricz[2], Zoltán Somogyi[2], Milan Koreň[3]

[1] *National Forest Centre – Forest Research Institute Zvolen, T. G. Masaryka 2175/22, 960 01 Zvolen, Slovak Republic*
[2] *National Agricultural Research and Innovation Centre – Forest Research Institute, 9600 Sárvár, Várkerület 30/A., Hungary*
[3] *Technical University in Zvolen, Faculty of Forestry, T. G. Masaryka 2117/24, 960 53 Zvolen, Slovak Republic*

Abstract
The paper demonstrates the multipurpose application of the normalized difference vegetation index (NDVI) derived from MODIS products for forest monitoring across the Central-European macro-region Slovakia and Hungary (i.e., the Western Carpathians and Pannonian basin). Relationships between forest dynamics and NDVI were analysed and used for determining the onset of phenophases in spring and autumn and for the assessment of forest growth and health condition. To identify the phenophases, the NDVI profile during the year was established by fitting a double logistic sigmoid function to data and phenological metrics were developed based on the calculated extreme values of the sigmoid function and its derivatives. According to our analyses, leaf unfolding and leaf fall were significantly delayed or advanced in 2018 with the increase of altitude and latitude ($p < 0.01$). The longitudinal aspect was significant only in the autumn phenophase with earlier onset of leaf fall towards to the east. The duration of the growing season varied extensively within the region, mainly according to altitudinal and latitudinal occurrence of beech forests. Positive associations between annual tree-ring width and standardized summer NDVI were found for conifers at local scale. The highest correlation period was between July 12 and August 12 as the most critical periods for forest growth. Slight positive correlation can be observed during March – April that could be associated with the varying start of the growing seasons. In the forest health study, whereas NDVI values could well identify the location and extent of a recent forest damage due to a combination of snow break and wind break, an urgent demand for more detailed field data was obvious.

Key words: MODIS; NDVI; forest phenology; growing season; tree ring; health condition

Editor: Michal Bošeľa

1. Introduction

Widespread abiotic and biotic disturbances started to occur with increasing frequency in Europe in the last decades (e.g. Lindner et al. 2014), including central European countries (Koltay 2006; Hirka 2018; Barka et al. 2018). The detoriation of forest health condition due to climate change and their possible adverse consequences in Central Europe (e.g. Somogyi 2016) are among the drivers in the development of remote-sensing based forest monitoring systems in this region.

Forest condition and plant phenology estimation over continuous spatial and temporal domains are essential for quantifying climate change impacts on forests and for understanding of vulnerability of forest ecosystems and socio-economic systems. Monitoring and research programs using such estimation are also the basis for suggestions of possible adaptation measures (e.g. Kovats et al. 2014). Satellite remote sensing seems to be an effective tool for this type of research. The advantages of using satellite sensors are the large spatial extent and high frequency of data collection, usually complemented with higher spectral resolution when compared with airborne sensors. Moreover, open access to satellite data with moderate or high resolution greatly increased their usage (Wulder et al. 2012), including forestry monitoring.

The conditions for monitoring forest health and phenology noticeably improved after the launch of the Terra and Aqua satellites (NASA Earth Observation System Satellites), equipped with the MODIS spectroradiometer (Moderate Resolution Imaging Spectroradiometer). The instrument collects data in 36 spectral bands, with wavelength ranging from 400 to 1 450 nm, at spatial resolutions from 250 m to 1 000 m (Justice et al. 2002). The most frequently used vegetation indices (i.e., the combi-

*Corresponding author. Ivan Barka, e-mail: ivan.barka@nlcsk.org

nation of spectral values of two or more bands designed to enhance the contribution of vegetation properties) are the normalized difference vegetation index (NDVI) and the enhanced vegetation index (EVI), especially in broadleaf forests (e.g. Beck et al. 2006; Heumann et al. 2007; Soudami et al. 2008; Hmimina et al. 2013).

Due to their moderate spatial resolution, it was questionable whether the MODIS data products could be used for forest monitoring at regional or even local scales. However, several studies from Central Europe exist which successfully utilize MODIS data for detection of stand-level intraseasonal climatic stress (Hlásny et al. 2015), forest damage (Bartold 2012) or continuous monitoring (Somogyi et al. 2018). This latter system (called TEMRE in Hungarian) was implemented for observing forest vitality related to environmental changes and describes forest health state by a standardized NDVI which is a measure of the intensity of photosynthetic activity, relative to a long-term local average.

Another possibility of using MODIS data for forest monitoring is to analyse the MODIS-based NDVI in combination with tree-ring chronologies. Tree-ring width is a widely used proxy for tree vitality (Fritts et al. 1971), and its relations to climate and extreme events, such as drought, are well recognized (Dobbertin 2005). The phenomena was studied in the south-western part of Hungary (Móricz et al. 2018) where the stands of Black pine (*P. nigra* Arn. var. *austriaca*) suffered from extreme droughts during the last decades. This latter study has found that the observed NDVI anomalies were in rough coincidence with remarkable growth reductions of trees due to drought conditions. However, no robust conclusions could be drawn due to the scarce availability of surface reflectance images of Landsat.

The seasonal variability of vegetation indices is related to phenology. Several approaches are available for modelling such variability, e.g. piecewise logistic functions (Ganguly et al. 2010), an adaptive Savitzky-Golay filter, asymmetric Gaussians function (Eklundh & Jönsson 2015), double logistic sigmoidal function (Fisher & Mustard 2007; Soudami et al. 2008) and its modification (Hmimina et al. 2013). During the last decade, phenology dynamics were analysed at pan-European level or at the level of European climatic zones (Delpierre et al. 2009; Hamunyela et al. 2013; Fu et al. 2014; Garonna et al. 2014; Jin et al. 2019). The research studies confirmed a general trend of extension of season duration due to its earlier onset and later end, although extensive variations in this trend were observed within and between climatic zones and landscape types.

Clearly, a more detailed macro-regional research is needed for a better understanding of how forests respond to changing environmental conditions. The main aim of this paper is to verify the applicability of MODIS-based NDVI for the detection and description of forest dynamics and forest conditions in Central European Region on the example of Slovakia and Hungary. The paper presents an analysis of the relationship between tree-ring chronologies and NDVI, field-based data on forest damages with NDVI in Bükk Mountains (Hungary), and the phenophases of beech stands based on the respective NDVI profiles for macro-region of the Carpathian Mountains and the Pannonia lowland for the year 2018.

2. Materials

2.1. Study area

The research was conducted within forests dominated by European beech (*Fagus sylvatica* L.) in Slovakia and Hungary. For the analysis of the phenological aspect, the minimum proportion of beech within the 250 × 250 m MODIS pixels was 50%. The total number of analysed pixels was 33 513, covering an area of 209 456 ha (Fig. 1A). Most of the beech stands extend between 200 and 1 100 m a. s. l. with average of 517 m.

Tree-ring analysis was done using samples from the Keszthely Mountains in south-western Hungary (46.83° N, 17.35° E, 200–400 m a. s. l. Fig. 1B). The spatial distribution of Black pine stands showed great similarity in growing and stand conditions such as shallow rocky soils with relatively little available water storage capacity and high crown closure.

The comparison of the MODIS-based assessment of forest health state with terrestrial observations was conducted in the Bükk Mountains in North-East of Hungary (Fig. 1C). In this region, a significant snow break, associated with a wind-fall and wind break events, caused forest damages on 4 409 ha of forests in April 2017 (Hirka 2018). The area is dominated by European beech (*Fagus sylvatica* L.) and Sessile oak (*Quercus petraea* (Matt.) Liebl.). The area has a cool and humid climate with average annual temperature below 8 °C, average precipitation 700 – 800 mm per year, typical soil types Luvisols, Cambisols and Rendzinas, and thickness rooting depth of more than 60 cm.

2.2. MODIS data

The phenological study was based on the MOD09 and MYD09 products (collection 6, United State Geological Survey, URL: http://e4ftl01.cr.usgs.gov). The MOD/MYD09GQ spectral bands 1 and 2 (centered at 648 nm and 848 nm) were used to derive the vegetation index NDVI at 250 m resolution. The *1km Reflectance Data State QA* layer from MOD/MYD09GA products was used for describing the quality of the products, particularly for cloud cover masking. Despite the potentially adverse effect of anisotropic reflectance of the vegetation on the use of MODIS daily products (Ju et al. 2011), we used the MOD/MYD09 because of spatial resolution and the necessity to capture immediate vegetation dynamics. Franch et al. (2013) claim that the effect of surface

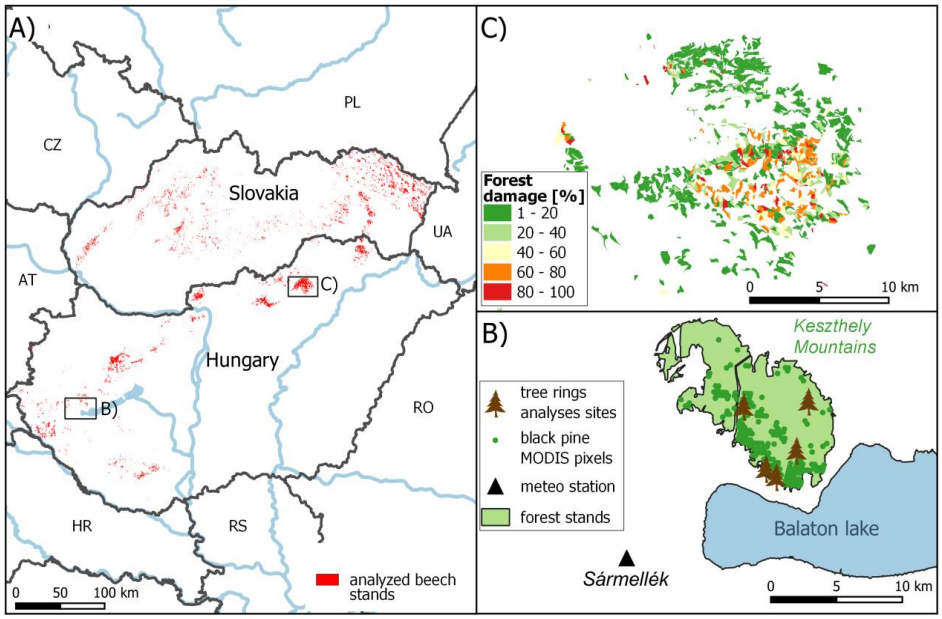

Fig. 1. A) The distribution of beech dominated pixels across Slovakia and Hungary. B) Study site in the Keszthely Mountains for a comparison of climatic indices and radial increment with the NDVI values. C) Study site in the Bükk Mountains for a comparison of field-based forest health assessment with the NDVI values; a map of the field-based forest damage frequency in 2017.

anisotropy in the red and infrared band of MODIS data barely influence NDVI estimation, obtaining RMSE of around 1%.

The TEMRE system is based on the MOD13Q1 – MODIS/Terra Vegetation Indices 16-Day L3 Global 250m SIN grid product (downloaded from the same URL as above), which is a 16-day NDVI composite. In the case of the tree-ring study, MODIS NDVI pixels were filtered from TEMRE (in total, 217 pixels) for correlation analysis that were covered dominantly (> 50%) by Black pine forests with age between 30 and 60 years and shallow soil depth (< 60 cm).

2.3. Meteorological data

Daily meteorological data (temperature, precipitation) were used in tree-ring analyses. Data were obtained for the period 1999 – 2016 from the nearest Keszthely (Sármellék) station (Hungarian Meteorological Service), located about 10 – 15 km from the study sites (Fig. 1B). The standardized precipitation index (SPI) and the standardized precipitation–evapotranspiration index (SPEI) were calculated on the monthly scale that was averaged to seasonal scale for correlation with growth (Vicente-Serrano et al. 2010). SPI is based solely on long-term precipitation data while SPEI is a multi-scalar drought index that allows the monitoring of water availability over various timescales using the monthly difference of precipitation and potential evapotranspiration. Both drought indices were computed using the SPEI package of the R software.

2.4. Tree ring chronologies

Tree-ring-width chronologies were established at the five selected sites in the Keszthely Mountains, considered representative for the region (Fig. 1B, Móricz et al. 2018). At each site, 12 living dominant Black pine trees were cored at 1.3 m height using a Pressler increment borer (Haglöf, Långsele, Sweden). Since we were interested in the mean chronology of the sites, a single core per tree was considered representative of that tree for dendrochronological analyses. Tree-ring widths were measured on scanned images (1 200 dpi) in WinDENDRO environment (Regent Instruments, Canada) with a resolution of 0.001 mm. Cross-dating was statistically checked using the program COFECHA (Holmes 1983). To remove age-related growth trends each cross-dated ring width series was detrended with a negative exponential curve (Fritts 1976) using the program ARSTAN (Cook 1985). With regard to the modest autocorrelation checked by the Akaike criterion (AIC), a standard version of chronologies was calculated as bi-weight robust mean of the individual series. The signal strength of the index series was checked using the expressed population signal (EPS) statistics (Wigley 1984).

The high correlations (0.78 – 0.90) of standardized chronologies among the sites allowed using the mean chronology of the five sites (46 – 60 trees in total, depending on the number of available trees) to calculate correlations with climate indicators and NDVI.

2.5 Field forest damage data

As field-based reference for forest damages (Fig. 1C), data from the Hungarian National Forest Damage Registration System (Nébih 2018) was used. This system is run by the NFCSO Forestry Department and the NARIC Hungarian Forest Research Institute. In total, 4 409.11 hectares of stands with various degrees of late frost damage were registered in 1 090 forest sub-compartments. The average damage, measured by the number of affected trees in percent of all trees, was 26.5% (Nébih, 2018).

3. Methods

3.1. Phenology analysis

3.1.1. MODIS quality analysis for phenological research

The quality of downloaded MOD09/MYD09 images was evaluated on image-level and pixel-level. The value of the spectral reflectance of each pixel is partly influenced by the spectral properties of the adjacent pixels (Townshend et al. 2000). This may increase the variability of the reflectance values. The pixels on the boundary between forest stands and other land cover classes were excluded from the analyses in order to minimize the variability of reflectance values.

Another criterion for the selection of appropriate images was the satellite position in relation to Slovakia and Hungary during data collection. Since the MODIS tracks are stable with 16-day repetitions, we could identify that there are 6 images in-nadir position related to Slovakia; 4 images in close-to-nadir position and 6 images in off-nadir position. Off-nadir images were completely excluded from downloading. Thus, we reduced the effect of anisotropic reflectance and achieved the spatial resolution close to 250 m. As the viewing angle increases, the actual ground pixel size increases continuously off-nadir both in along-track and along-scan directions (Kristof & Pataki 2009).

In addition to the visual inspection of image quality, we analysed the *1km Reflectance Data State QA* layer present in the MOD09GA/MYD09GA products. The quality information of individual pixels is encoded as values of individual bits in 16-bit integers. MOD/MYD09 product quality description and an optimal combination of bit values were applied in deciding on the inclusion or exclusion of a pixel in the analysis. Based on the data from the quality dataset, we selected pixels with the following bit values: 8, 72, 76, 136, 140, 200 and 8200. Other pixel values were treated as no data. This ensured that only the best quality data, not influenced by detected cirrus clouds, clouds, cloud shadows, snow or fires, were analysed.

Reflectance values (i.e., DN values) of the selected pixels underwent a final quality check. The arithmetic mean (x) and standard deviation (SD) of DN values were calculated for each selected image from the database. A pixel was included in the analysis if its value ranged within $x \pm 2$ SD. The pixels outside this range were assigned a bit value of zero.

After applying the rules for image and pixel selection, the 68 images of the MODIS images were used for the analyses in year 2018.

3.1.2. Constructing a phenological model

Modelling phenology entails predicting the onset of the main phenological events through the analysis of NDVI during the year. The raw NDVI data were smoothed with sigmoidal logistic curve (Fisher & Mustard 2007) using the PhenoProfile software (Bucha & Koreň 2014):

$$v(t) = v_{min} + v_{amp}\left(\frac{1}{1+e^{m_1-m_2 t}} - \frac{1}{1+e^{m_3-m_4 t}}\right) \quad [1]$$

Where $v(t)$ is NDVI observed at day of year (DOY) t; v_{min} and v_{amp} parameters correspond to the minimum value of the vegetation index (NDVI) and amplitude (maximum minus minimum); m_1 and m_2 parameters control the shape and slope of the curve of the ascending (spring) phase, and m_3 and m_4 parameters control the descending (autumn) phase.

In this study, v_{min} and v_{amp} parameters were not subject to formula [1] calculation, but they were used as constants. We used the values for beech: $v_{min} = 0.429$ and $v_{amp} = 0.497$ for spring phase and $v_{min} = 0.499$ and $v_{amp} = 0.417$ for autumn phase. The v_{min} and v_{amp} parameters for the spring phase have been taken from Bucha & Koreň (2014). There were 27 images from the spring period (DOY 92 to 181) used as an input in derivation of these 4 parameters. The autumn phase v_{min} and v_{amp} values were derived iteratively based on the minimum RMS error of equation [1]. The baseline values were identical to those of the spring phase. The values of v_{min} was gradually increased and v_{amp} decreased in steps of 0.01. The input set for autumn phenophase consisted of 37 images from the summer and autumn periods (DOY 181 to 321).

Calculation of $m_1 - m_4$ parameters was done separately for each pixel with beech occurrence. The extremes of the first and second derivatives of the function [1] were used to determine the approximative onset of the new phenological phase.

The period of the maximal rate of change corresponds with the inflection point (IP) in spring or autumn phenological phases (Fig. 2, Table 1). Other significant points of the function represent the days of maximal acceleration and maximal deceleration in spring and autumn phases, and these correspond to the local extremes of the second derivative of the sigmoid function.

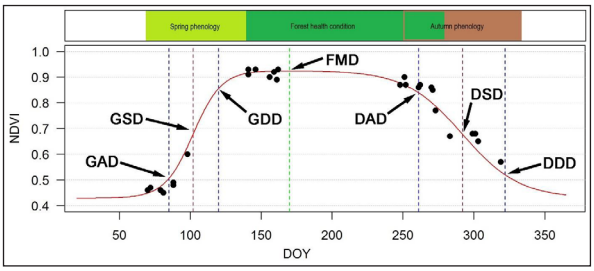

Fig. 2. The typical course of NDVI values of beech stands (dots) modelled by the sigmoid logistic curve [1] with the onsets of phenophases. Explanation of phenological metrics is given in Table 1.

Table 1. Satellite-derived phenological metrics based on the sigmoidal logistic curve and corresponding approximative vegetative phenophase.

GAD	Maximum (maximum acceleration) of the second derivative of the function in the spring phase ~ bud break onset
GSD	Extreme of the first derivative of the function in the spring phase (spring inflection point) ~ leaf unfolding onset
GDD	Minimum (maximum deceleration) of the second derivative of the function in a spring phase ~ end of leaf unfolding
FMD	Maximum of a phenological curve ~ Full foliage
DAD	Maximum (maximum acceleration) of the second derivative of the function in an autumn phase ~ leaf yellowing onset
DSD	Extreme of the first derivative of the function in an autumn phase (autumn inflection point) ~ leaf fall onset
DDD	Minimum (maximum deceleration) of the second derivative of the function in the autumn phase ~ the end of leaf fall

3.1.3. Statistical evaluation of phenological data

The onset of the main phenophases in beech stands was expressed by median values of the day of the onset for year 2018. Intra-annual variation was expressed by the 5 – 95% quantile.

Multiple linear regression analyses were applied in analysing spatial variation of GSD (DSD) in 2018 as the function of altitude, latitude and longitude.

Based on previous studies (Pavlendová & Snopková 2014), the thresholds for SOS and EOS (start and end of growing season) were set to GSD and DSD. The duration of the growing season (GS) was then calculated for each pixel as the difference between the day of the onset of leaf fall and the onset of leaf unfolding, i.e. GS = DSD − GSD.

3.2. Comparison of climatic indices and radial increment with the NDVI values

Correlation of the standardized NDVI at fine (250 m) spatial resolutions with two climatic indices was analysed and compared with the ring width time-series for different timescales of NDVI for the period 2000 – 2016. To assess the relationships among climate, tree growth and NDVI, Pearson correlations were used. Seasonal (3-months) averages of the SPI and SPEI were correlated with the standardized mean NDVI of the summer months (June – August) from spring of the previous year until summer of the actual year of ring formation. Correlation between the standardized tree ring chronology and standardized NDVI were calculated for each 16-day period of image acquisition (in total 23 during the year) over each mean standardized NDVI of the preceding 23 cycles of 16-day periods.

3.3. Forest health assessment

3.3.1. Construction of a model for forest health assessment with the NDVI values

Since the absolute values of the photosynthetic activity depend heavily on the seasonality and many other factors, standardized NDVI values were calculated that are much better for detecting health anomalies in time and space. For the mean date of any 16-day period, this standardized NDVI, Z_{NDVI}, is calculated the following way (Peters et al. 2002):

$$Z_{NDVI} = \frac{NDVI - \overline{NDVI}}{\sigma_{NDVI}} \quad [2]$$

where $\overline{NDVI}$ is the mean NDVI, and σ_{NDVI} is the standard deviation of NDVI values calculated from all the NDVI values of the entire 2000 – 2018 time series for the given date. Using the Z_{NDVI} values, the forest health state is classified in TEMRE using codes according to the anomaly from the mean: < −2 (possible serious vitality problem); −2 – −1 (possible moderate vitality problem); −1 – 0 (possible slight vitality problem); 0 – +1 (slightly better than normal state); > +1 (moderately better than normal state). Below zero Z_{NDVI} values, i.e. where the actual NDVI value is less than the long-term average, might indicate a forest health issue predominantly in larger blocks of forests if the anomaly lasts for a longer period.

In the forest health study based on the TEMRE system, the 16-day standardized NDVI layers from April to October (i.e., DOY 129 to 273) in the year of the damage 2017 and in the subsequent year 2018 were used. Maps from July 2015 and 2016 served as a reference for healthy forest state.

For tree-ring analyses, the 16-day periods with more than half of the pixels missing were (mainly in the winter seasons). Additionally, a manual quality control procedure was applied, aimed at removing NDVI values that were inconsistent with the expected annual NDVI cycle (Bruce et al. 2006). Finally, the missing data were linearly interpolated using the zoo package of the R software and the corresponding standardized NDVI values were calculated with the same procedure as used in the TEMRE system.

3.3.2. Comparison of field-based forest health assessment with the NDVI values

Forest damage data of the sub-compartments were aligned with the corresponding MODIS pixels by selecting the sub-compartment with the greatest spatial extent under the pixels. The standardized NDVI values were acquired from the images and the resulting dataset was further statistically analysed in MS Excel software from the viewpoint of damaged area distribution within standardized NDVI values.

4. Results

4.1. Phenological research – a leaf unfolding and leaf fall phenophase

The overview of the onsets of spring and autumn phenophases of beech stands in 2018 is given in Table 2.

Table 2. The onsets of spring and autumn phenophases of beech stands in 2018 (DOY).

	GAD	GSD	GDD	DAD	DSD	DDD
Mean	101.6	107.7	113.8	273.3	285.2	297.1
Std deviation	2.8	2.8	4.1	4.0	4.7	8.5
Median	102	108	113	274	284	294
5% quantile	97	104	109	266	280	287
95% quantile	106	113	122	278	295	314
Duration	9	9	9	12	15	27

The average of the onset of leaf-unfolding in 2018 was DOY 108, expressed as median value. The duration of the GSD phenophase occurred in 2018, lasting 9 days from DOY 97 to 106. The average onset of leaf-fall in 2018 was DOY 284. The duration of the leaf fall phenophase was 15 days from DOY 280 to 295.

4.2. Temporal and spatial aspects of the onset of phenophases

The maps graphically depicting the spatial-temporal variation of the beginning of leaf unfolding and leaf fall of beech stands in macro-region Slovakia and Hungary, expressed as GSD and DSD, are presented in Fig. 3. The duration of the growing season is illustrated in Fig. 4. To enhance the visual perception, a median filter with the dimensions of 3 × 3 pixels magnified the number of pixels in all figures. The mean duration of the growing season (GS) for the whole macro-region was 177.6 days with standard deviation ± 6.66 days. The median value was 176 days and the duration of GS varied from 165 to 196 days (range 31 days), expressed as the 1 – 99th percentile.

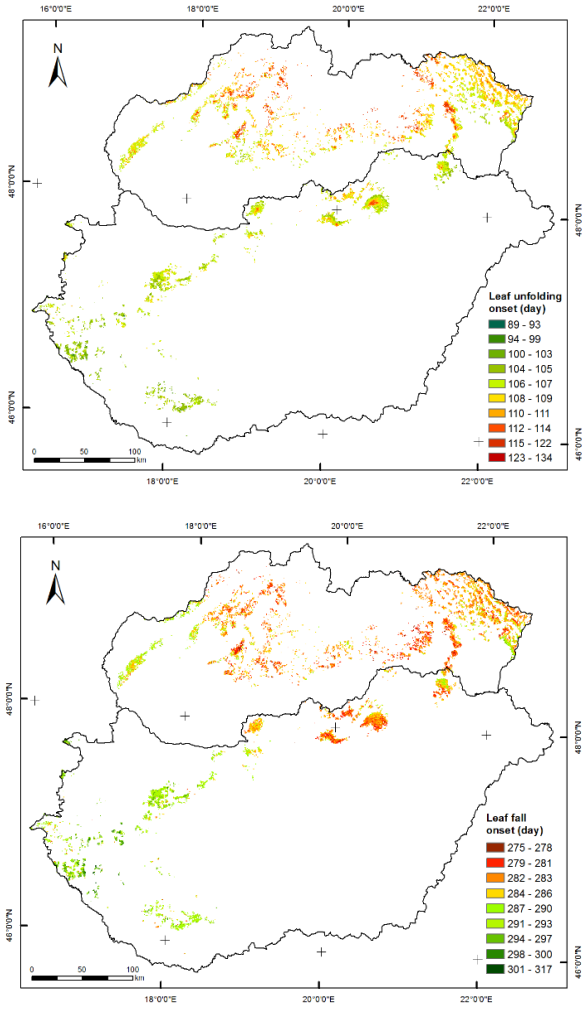

Fig. 3. GSD (left) and DSD (right) – DOY of the onset of leaf-unfolding and leaf-fall in 2018.

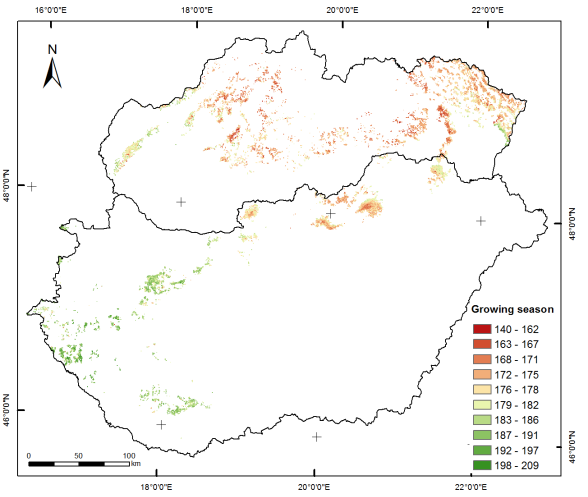

Fig. 4. Duration of the growing season 2018 in days: GS = DSD – GSD.

4.3. Altitudinal and geographical aspects of the onset of phenophases

The results of multiple and simple regression analysis between the onset of GSD, DSD and the altitude and latitude and longitude are given in Table 3.

Table 3. Regression equations and correlation for GSD and DSD.

Multiple linear regressions:
GSD = 100.62 + 0.0082 * Altitude + 0.0026 * Latitude r = 0.74; Std. Error of estimate (SEE) = 1.91; p < 0.01; n = 32 610
DSD = 296.04 – 0.0079 * Altitude – 0.0029 * Latitude – 0.0030 * Longitude r = 0.71; Std. Error of estimate (SEE) = 3.28; p < 0.01; n = 32 610
Simple linear regressions:
GSD = 102.31 + 0.0107 * Altitude r = 0.67; Std. Error of estimate (SEE) = 2.09; p < 0.01; n = 32 610
GSD = 102.78 + 0.0046 * Latitude r = 0.57; Std. Error of estimate (SEE) = 2.31; p < 0.01; n = 32 610
GSD = 105.65 + 0.0018 * Longitude r = 0.36; Std. Error of estimate (SEE) = 2.63; p < 0.01; n = 32 610
DSD = 291.55 – 0.0123 * Altitude r = −0.49; Std. Error of estimate (SEE) = 4.05; p < 0.01; n = 32 610
DSD = 294.14 – 0.0080 * Latitude r = −0.62; Std. Error of estimate (SEE) = 3.64; p < 0.01; n = 32 610
DSD = 290.80 – 0.0048 * Longitude r = −0.59; Std. Error of estimate (SEE) = 3.74; p < 0.01; n = 32 610

Remarks: onsets of GSD and DSD are expressed in DOY (day of year); Altitude is expressed in meters above sea level. Latitude and Longitude are expressed in pixel order from 1 to 1 786 resp. from 1 to 2 151. One pixel represent dimension 250 × 250 m.

Concerning GSD, our analysis revealed a statistically significant correlation ($r = 0.74$; $p < 0.01$) between the onset of GSD (leaf unfolding) and the altitude and latitude. The estimated latitudinal shift (delay in onset) was 1.05 day per 100 km to the North, at a steady altitudinal shift of 0.82 day per 100 m. The longitudinal shifts was not significant ($p > 0.05$).

Concerning DSD, the analysis revealed a statistically significant ($r = 0.71$; $p < 0.01$) earlier leaf fall onset with altitude, latitude, and longitude. The estimated latitudinal shift was –1.17 day per 100 km to the North (early onset), whereas the longitudinal shift was approximately −1.20 day per 100 km to the East at a steady altitudinal shift of −0.79 day per 100 m.

4.4. Radial increment and climate indices vs NDVI values

The quality-checked NDVI time series showed a clear seasonal fluctuation for the selected Black pine sites with a slight but not significant decreasing trend (*Mann-Kendall tau = −0.0344, p = 0.286*) (Fig. 5A). The derived standardized NDVI is more informative for detecting NDVI anomalies such as the long and deep negative period after the drought event in 2011 – 2012 (Fig. 5B).

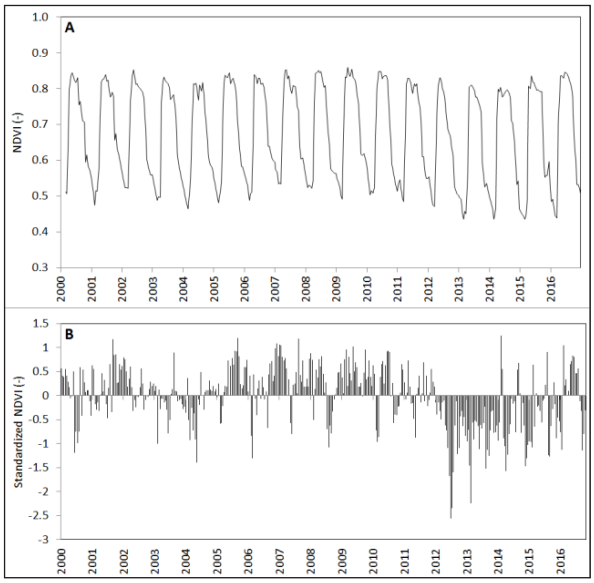

Fig. 5. Time series of row NDVI (A) and standardized NDVI (B) for the period 2000 – 2016.

The correlation between the mean summer standardized NDVI and corresponding seasonal drought indices was highest ($r = 0.56$ and 0.55) and significant ($p < 0.05$ one-tailed t test) with the current summer SPI and SPEI values respectively (Fig. 6.). The mean of spring and summer SPI and SPEI value also showed significant correlation with NDVI ($r = 0.5$ and 0.53, $p < 0.05$ one-tailed t test). Both drought indices demonstrate that precipitation was a good indicator of NDVI anomalies.

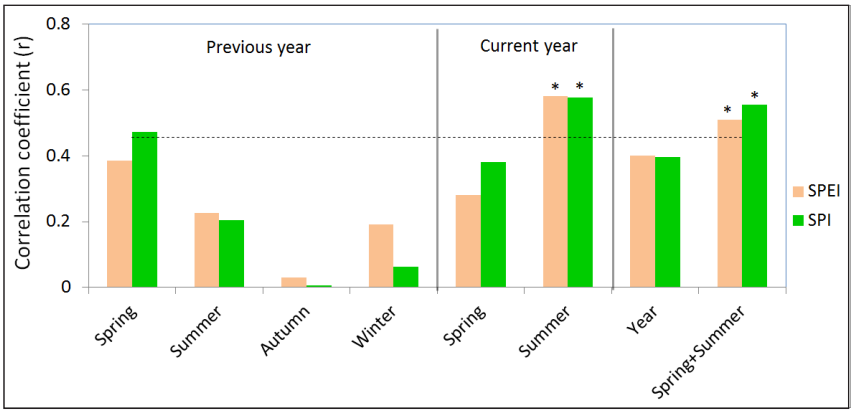

Fig. 6. Correlation between the mean summer standardized NDVI and corresponding seasonal drought indices.

The NDVI from the beginning of June until the end of August (periods 11 – 15) and cumulating up to period 15 showed positive relationships with the corresponding annual tree-ring widths (Fig. 7).

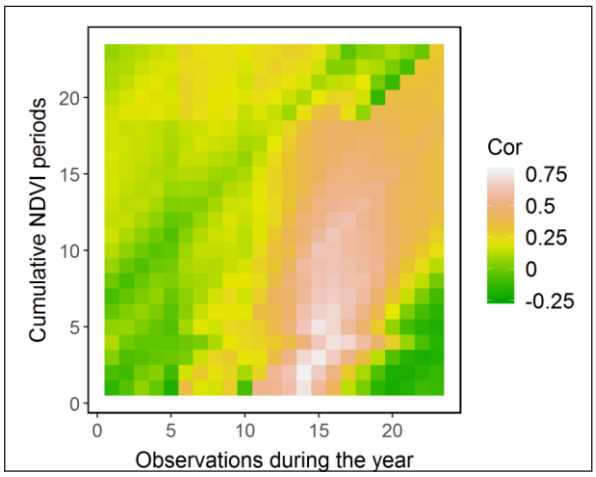

Fig. 7. Pearson correlation coefficients between time series of tree-ring width index and NDVI for different temporal scale (y–axis). The x–axis shows the 23 periods of the 16-day MODIS composites during a year.

The highest correlation period (r = 0.77) was between July 12 and August 12 as the most critical periods for forest growth. Slight positive correlation (r up to 0.36) can be observed during March-April that could be associated with the varying start of the growing seasons.

4.5. Field-based assessment of forest health vs NDVI values

The standardized NDVI of the area showed that forest vitality declined remarkably from the preceding years 2015 – 2016 to 2017, i.e., after the snow break occurred. The substantially damaged forest areas (Z < −2) expanded from 1.4% to 10.1% during this period (Fig. 8).

According to the NDVI images (Fig. 8), the damages affected mostly the higher regions of the Bükk Mountains over 400 m above sea level. The most severely damaged area was not in the zone of the highest peaks but in the north-western part of the mountain.

The 16-day standardized NDVI time series from May of 2017 until the end of growing season 2018 showed the abrupt large depression of NDVI after the calamity event (i.e., early May, Fig. 9).

This anomaly was mainly caused by the strong late frost that induced a prompt leaf loss of the trees, especially for beech. The standardized NDVI (Z NDVI) was still below the mean values for the rest of the year, but the negative deviation of Z NDVI remained moderate (< −1). This could be explained by the field observations that revealed that the trees that had lost their leaves formed new shoots later during the spring of 2017. In 2018 only small patches of negative Z NDVI were left, demonstrating that the forests could recover almost everywhere from this event with the new vegetation season, except the heavily damaged areas where sanitary cutting of the forests was conducted.

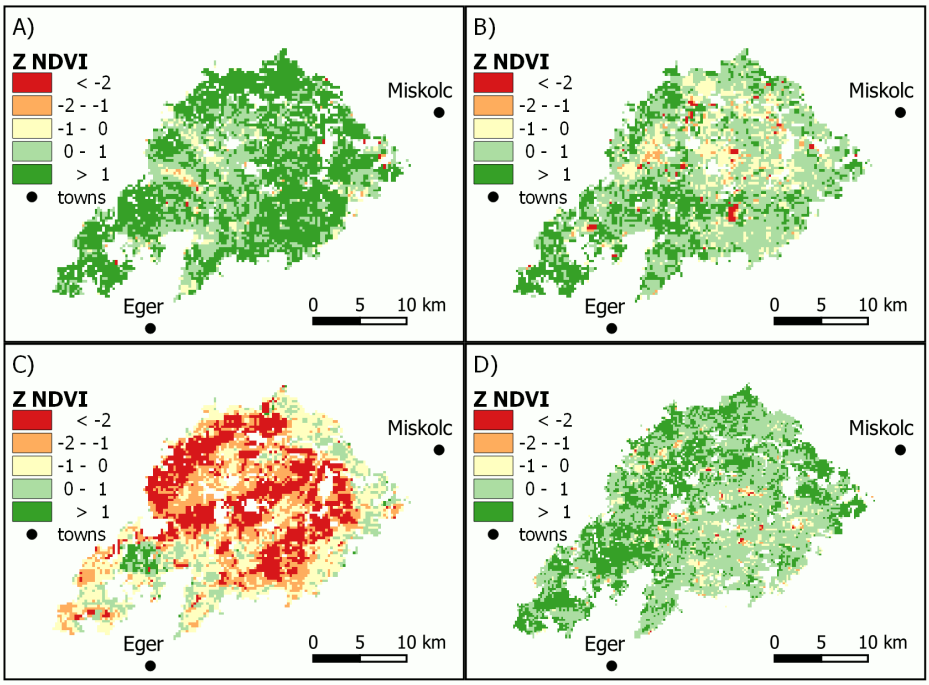

Fig. 8. Forest state of Bükk Mountains based on TEMRE Z NDVI (day/month/year).
A) 18/7/2015. B) 18/7/2016. C) 16/5/2017. D) 19/8/2018.

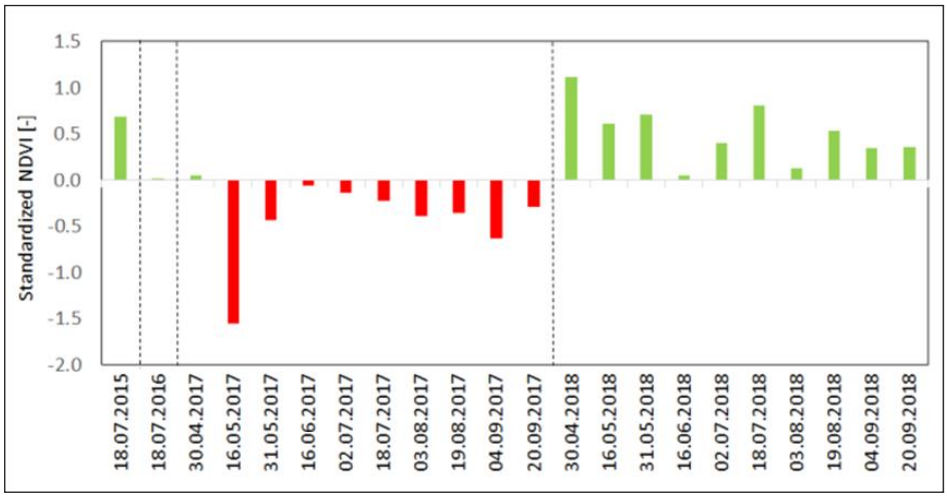

Fig. 9. Time series of standardized NDVI for the Bükk Mountains (2017–2018 and two observation dates for 2015 and 2016 as references).

5. Discussion

5.1. Comparison with regional phenological studies

Regarding the altitudinal gradient of beech forest in Slovakia, Schieber et al. (2013) during the period of 2007 – 2011 discovered that the phenological gradient for spring phenophases ranged from +2.83 to +3.00 days per 100 m and from −1.00 to −1.78 days per 100 m for autumn phenological phases. Positive value means later, negative value earlier onset.

Regarding the altitudinal gradient of phenophases, Bucha & Koreň (2017) confirmed trends similar to ours in a study focused on phenological temporal and spatial changes of beech forest in Slovakia in period 2000 – 2015. In their study, the multiple linear regression analyses revealed altitudinal shift of GSD and DSD onset of 1.6 (−0.6) day per 100 m, whereas latitudinal shifts were 3.7 (0.83) day per 100 km to the North and the longitudinal shifts were approximately 0.24 (−0.23) day per 100 km to the East.

Our results, related to GSD onset in 2018, are consistent with both regional studies in term of +/− trends. However, the estimated altitudinal GSD shift of 0.82 day per 100 m and latitudinal shift 1.05 day per 100 km to the North were moderate in comparison to the above-mentioned studies.

Concerning DSD, the estimated altitudinal shift of −0.79 day per 100 m confirmed the trends from previous studies; however, the longitudinal shift of −1.20 day per 100 km to the East was stronger.

A much broader extent of macro-regional analysis in the direction of latitude revealed that the latitudinal shift −1.17 per day 100 km to the North in study region was completely opposite to the trend observed in Slovakia in 2000 – 2015 period (0.83 day). This could be influenced by selecting just one year (i.e., 2018) or by broader analysed region.

The regression coefficients of the multiple linear regressions between the dependent and independent variables (GSD, DSD vs. altitude, latitude, longitude) are not directly comparable with those of simple linear regressions. In case of regional studies, the results underline the need to further study the complexity of the spatial variability of phenological events in relation to altitude and geographical location.

Phenological modelling in the presented study was based on Fisher & Mustard's (2007) definition of the date of leaf unfolding (leaf fall) as the date on which the sigmoid function reaches its half-maximum value. However, based on the comparison of our findings with those of our previous ones, we modified our approach. We found that NDVI values of beech forest in the period without leaves were different in spring and autumn. Moreover, the NDVI values were slightly lower than the maximum values in the end of summer period. Therefore, we performed the calculation of $m_1 - m_4$ parameters of formula [1] twice, once for deriving the spring phenophase and the second time for deriving the autumn phenophase with v_{min} and v_{amp} parameters different for each phase.

5.2. Tree-rings vs NDVI values

Tree-ring chronologies are not suitable for monitoring of forest growth over large areas due to the time-consuming work of tree-ring preparation (Vicente-Serrano et al. 2016). In contrast, the remotely sensed NDVI indicates the photosynthetic activity of the forest canopy can be used to estimate vegetation productivity (Lopatin et al. 2006). Although the inter-comparison of NDVI, drought indices and ring width index could lead to a better understanding of the response of a forest to recent climatic trends, results of such inter-comparisons still can be found in the literature only rarely (e.g. Camarero et al. 2015).

In general, the tree-ring width vs NDVI relations of the present study are comparable to those found for conifers in mid-latitudes in the Northern Hemisphere (Lopatin et al. 2006; Bhuyan et al. 2017; Kaufmann et al. 2008). A similar positive relationship between NDVI of June to August and conifer growth was found by Lopatin et al. (2006) and Bunn et al. (2013) for Siberia using NOAA AVHRR PAL and GIMMS NDVI data. Similarly, for North America, studies have reported positive associations between NDVI and conifer ring-widths for Canada (Berner et al. 2013).

A recent study of Bhuyan et al. (2017) used also the 250 m spatial resolution MODIS NDVI for correlating with tree-ring data of forests types in different climate zones of the Northern Hemisphere. They found that the growth of conifers in the temperate climate zone was in tight relationship with the NDVI of summer months with up to 10 cumulating periods. Their analysis was constrained by the fact that no further information about the forest sites (stand and site conditions) was available. In the present study, it was possible to use a pre-filtered database for the analysis despite the fact that it was spatially representative only for a small region.

The autumn and winter weather conditions of the preceding year had almost no effect on the NDVI of the next summer. This can be explained by the low soil water capacity of the selected sites that enhanced the importance of precipitation, as found also by Móricz et al. (2018).

5.3. Field-based forest health assessment vs NDVI values

Vitality loss might happen due to abiotic (snow break, windfall, leaf loss, heat, drought) or biotic causes (pests, pathogens) resulting in physiological deficiencies or leaf loss. If discolorations are detected on larger areas and are sustained over longer time (weeks or rather months), a field survey is essential to verify the satellite indicated issues and further explore the nature of the damage.

The low correlation between the ground-based damage data and the MODIS NDVI in our study may be explained by three major factors. First, the surveyed damaged area, and thus the amount of field data, available for analysis, was very low as there are still large areas with missing data due to inaccessible terrain. Second, the method used for aligning the ground-based field data to the corresponding MODIS pixels could only make use the area of the sub-compartments occupying under each of the MODIS pixels. This method might lead to bias since the shape of the sub-compartments is variable. Quite often, a number of sub-compartments with varying damage severity had to be attached to the same MODIS pixel. For that reason, we included only those MODIS pixels in the analyses whose area was covered by one or two forest sub-compartments. Inevitably, only a small fraction of original data was left for the analysis. Finally, field assessments showed a spatially very heterogenic distribution of forest damages even within the sub-compartments with numerous tree species. This reinforced using the importance of the selected methodology. Although an area-weighted approach could rectify some of the above issues, this would require more detailed input field measurements than what we had access to.

6. Conclusions

By focusing on a macro-region of Pannonian lowland and Western Carpathians, this paper demonstrated that the MODIS-based satellite applications in medium spatial resolution can be successfully used for regional assessment of forest health and phenological phases. Positive associations between annual tree-ring width and summer NDVI was found for conifers at local scale which confirmed the results of previous large-scale analysis.

Further modelling of regional phenology development is needed in order to provide a better explanation of spatial variations of phenological events, especially if the results are to be transferred into species selection practice in forest restoration (after planned logging or disturbances) in relation to forest adaptation to climate change. For a more successful study of forest health, an urgent demand for more detailed field data is obvious.

Acknowledgements

The collaborative research reported by the present study was conducted with the support by the Slovak Research and Development Agency under Grants APVV-15-0413 and APVV-16-0325, by the project ITMS "26220120069 Centre of excellence for decision support making in forest and landscape", funded by the Operational Programme Research and Development financed from the European Regional Development Fund, as well as the EMMRE monitoring program funded by the Hungarian Ministry of Agriculture. The authors thank the NFCSO Forestry Department for giving access to the Hungarian National Forest Damage Registration System data.

References

Barka, I., Lukeš, P., Bucha, T., Hlásny, T., Strejček, R., Mlčoušek, M., Křístek, Š., 2018: Remote sensing-based forest health monitoring systems – case studies from Czechia and Slovakia. Central European Forestry Journal, 64:259–275.

Bartold, M., 2012: Monitoring of forest damages in Poland and Slovakia based on Terra.MODIS satellite images. Geoinformation Issues, 4:23–31.

Beck, P. S. A., Atzberger, T. C., Høgda, K. A., Johansen, B., Skidmore, A. K., 2006: Improved monitoring of vegetation dynamics at very high latitudes: A new method using MODIS NDVI. Remote Sensing of Environment, 100:321–334.

Berner, L. T., Beck, P. S. A., Bunn, A. G., Goetz, S. J., 2013: Plant response to climate change along the forest-tundra ecotone in northeastern Siberia. Global Change Biology, 19:3449–3462.

Bhuyan, U., Zang, C., Vicente-Serrano, S. M., Menzel, A., 2017: Exploring Relationships among Tree-Ring Growth, Climate Variability, and Seasonal Leaf Activity on Varying Timescales and Spatial Resolutions. Remote Sensing, 9:526.

Bruce, L. M., Mathur, A., Byrd, J. D., Jr., 2006: Denoising and wavelet-based feature extraction of MODIS multi-temporal vegetation signatures. GIS science & Remote Sensing, 43:67–77.

Bucha, T., Koreň, M., 2014: Tvorba údajovej bázy a modelovanie fenológie lesných porastov. In: Bucha, T. (ed.): Satelity v službách lesa. Bratislava, SAP-Slovak Academic Press, 202 p.

Bucha, T., Koreň, M., 2017: Phenology of the beech forests in the Western Carpathians from MODIS for 2000–2015. iForest-Biogeosciences and Forestry, 10:537–546.

Bunn, A. G., Hughes, M. K., Kirdyanov, A. V., Losleben, M., Shishov, V. V., Berner, L. T. et al., 2013: Comparing forest measurements from tree rings and a space-based index of vegetation activity in Siberia. Environmental Research Letters, 8:1–8.

Camarero, J. J., Franquesa, M., Sangüesa-Barreda, G., 2015: Timing of drought triggers distinct growth responses in holm oak: implications to predict warming-induced forest defoliation and growth decline. Forests, 6:1576–1597.

Cook, E. R., 1985: A Time Series Analysis Approach to Tree-Ring Standardization. Ph.D. Thesis, University of Arizona, Tucson, AZ, USA, 5 August 1985.

Delpierre, N., Dufrêne, E., Soudani, K., Ulrich, E., Cecchini, S., Boé, J., François, C., 2009: Modelling interannual and spatial variability of leaf senescence for three deciduous tree species in France. Agricultural and Forest Meteorology, 149:938–948.

Dobbertin, M., 2005: Tree growth as indicator of tree vitality and of tree reaction to environmental stress: A review. European Journal of Forest Research, 24:319–333.

Eklundh, L., Jönsson, P., 2015: TIMESAT: A Software Package for Time-Series Processing and Assessment of Vegetation Dynamics. In: Kuenzer, C. et al. (eds.): Remote Sensing Time Series 22. Springer International Publishing, Switzerland, p. 141–158.

Fisher, J. I., Mustard, J. F., 2007: Cross-scalar satellite phenology from ground, Landsat and MODIS data. Remote Sensing of Environment, 109:261–273.

Franch, B., Vermote, E. F., Sobrino, J. A., Fédèle, E., 2013: Analysis of directional effect on atmospheric correction. Remote Sensing of Environment, 128:276–288.

Fritts, H. C., Blasing, T. J., Hayden, B. P., Kutzbach, J. E., 1971: Multivariate techniques for specifying tree-growth and climate relationships and for reconstructing anomalies in paleoclimate. Journal of Applied Meteorology, 10:845–864.

Fritts, H. C., 1976: Tree Rings and Climate. New York, NY, USA, Academic Press, 582 p.

Fu, Y. H., Piao, S., Op de Beeck, M. O., Cong, N., Zhao, H., Zhang, Y. et al., 2014: Recent spring phenology shifts in western Central Europe based on multiscale observations. Global Ecology and Biogeography, 11:1255–1263.

Ganguly, S., Friedl, M. A., Tan, B., Zhang, X., Verma, M., 2010: Land surface phenology from MODIS: Characterization of the Collection 5 global land cover dynamics product. Remote Sensing of Environment, 114:1805–1816.

Garonna, I., De Jong, R., De Wit, A. J. W., Mücher, C. A., Schmid, B., Schaepman, M. E., 2014. Strong contribution of autumn phenology to changes in satellite-derived growing season length estimates across Europe (1982–2011). Global Change Biology, 11:3457–3470.

Hamunyela, E., Verbesselt, J., Roerink, G., Herold, M., 2013: Trends in Spring Phenology of Western European Deciduous Forests. Remote Sensing, 5:6159–6179.

Heumann, B. W., Seaquist, J. W., Eklundh, L., Jönsson, P., 2007: AVHRR derived phenological change in the Sahel and Soudan, Africa, 1982–2005. Remote Sensing of Environment, 108:385–392.

Hirka, A., 2018: A 2017. évi biotikus és abiotikus erdőgazdasági károk, valamint a 2018-ban várható károsítások. Avaiable at: <http://www.erti.hu/hu/publikációs-hírek/731-prognózis-füzet-2018f>

Hlásny, T., Barka, I., Sitková, Z., Bucha, T., Konôpka, M., Lukáč, M., 2015: MODIS-based vegetation index has sufficient sensitivity to indicate stand-level intra-seasonal climatic stress in oak and beech forests. Annals of Forest Science, 1:109–125.

Hmimina, G., Dufrêne, E., Pontailler, J. Y., Delpierre, N., Aubinet, M., Caquet, B. et al., 2013: Evaluation of the potential of MODIS satellite data to predict vegetation phenology in different biomes: An investigation using ground-based NDVI measurements. Remote Sensing of Environment, 132:145–158.

Holmes, R. L., 1983: Computer-assisted quality control in tree-ring dating and measurement. Tree-Ring Bulletin, 43:69–78.

Jin, H., Jönsson, A. M., Olsson, C. et al., 2019: New satellite-based estimates show significant trends in spring phenology and complex sensitivities to temperature and precipitation at northern European latitudes. International Journal of Biometeorology, 6:763–775.

Ju, J., Roy, D. P., Shuai, Y., Schaaf, C., 2011: Development of an approach for generation of temporally complete daily nadir MODIS reflectance time series. Remote Sensing of Environment, 114:1–20.

Justice, C. O., Townshend, J. R. G., Vermote, E. F., Masuoka, E., Wolfe, R. E., Saleous, N. et al., 2002: An overview of MODIS land data processing and product status. Remote Sensing of Environment, 83:3–15.

Kaufmann, R. K., D'Arrigo, R. D., Paletta, L. F., Tian, H. Q., Jolly, W. M., Myneni, R. B., 2008: Identifying climatic controls on ring width: The timing of correlations between tree rings and NDVI. Earth Interactions, 12:1–14.

Koltay, A., 2006: Az erdők egészségi állapotának változásai az erdővédelmi monitoring rendszerek adatai alapján. Tájökológiai lapok, 2:327–337.

Kovats, R. S., Valentinim, R., Bouwer, L. M., Georgopoulou, E., Jacob, D., Martin, E. et al., 2014: Europe. In: Climate Change 2014: Impacts, Adaptation, and Vulnerability. Part B: Regional Aspects. Contribution of Working Group II to the Fifth Assessment Report of the Intergovernmental Panel on Climate Change. Cambridge University Press, Cambridge, United Kingdom and New York, NY, USA, p. 1267–1326.

Kristof, D., Pataki, R., 2009: Novel vector-based preprocessing of MODIS data. In: Maktav, D. (ed.): Remote Sensing for a Changing Europe. IOS Press, Amsterdam, 649 p.

Lindner, M., Fitzgerald, J. B., Zimmermann, N. E., Reyer, C., Delzon, S., van der Maaten, E. et al., 2014: Climate change and European forests: What do we know, what are the uncertainties, and what are the implications for forest management? Journal of Environmental Management, 146:69–83.

Lopatin, E., Kolström, T., Spiecker, H., 2006: Determination of forest growth trends in Komi Republic (northwestern Russia): Combination of tree-ring analysis and remote sensing data. Boreal Environment Research, 11:341–353.

Móricz, N., Garamszegi, B., Rasztovits, E., Bidló, A., Horváth, A., Jagicza, A. et al., 2018: Recent Drought-Induced Vitality Decline of Black Pine (*Pinus nigra* Arn.) in South-West Hungary–Is This Drought-Resistant Species under Threat by Climate Change? Forests, 9:414.

Nébih, 2018: Országos Erdőkár Nyilvántartási Rendszer (OENYR) útmutató. Avaiable at: <http://portal.nebih.gov.hu/documents/10182/1047730/Erdővédelmi+kárbejelentő_Útmutató_új_20180604.pdf/96c53f3a-89ca-967f-f40a-98b059115fad>

Pavlendová, H., Snopková, Z., 2014: Validácia nástupu fenologických udalostí bukových porastov. In: Bucha, T. (ed): Satelity v službách lesa. Bratislava, SAP-Slovak Academic Press, 202 p.

Peters, A. J., Walter-Shea, E. A., Andrés Viña, L. J., Hayes, M., Svoboda, M. D., 2002: Drought monitoring with NDVI-based standardized vegetation index. Photogrammetric Engineering and Remote Sensing, 1:72–75.

Schieber, B., Janík, R., Snopková, Z., 2013: Phenology of common beech (*Fagus sylvatica* L.) along the altitudinal gradient in the Slovak Republic (Inner Western Carpathians). Journal of Forest Science, 4:176–184.

Somogyi, Z., 2016. Projected effects of climate change on the carbon stocks of european beech (*Fagus sylvatica* l.) forests in Zala County, Hungary. Lesnícky časopis - Forestry Journal, 62:3–14.

Somogyi, Z., Koltay, A., Molnár, T., Móricz, N., 2018: Forest health monitoring system in Hungary based on MODIS products. In: Molnár, V. É. (ed.): Theory Meets Practice in GIS; Proceedings of the 9. TérinformatikaiKonferenciaésSzakkiállítás, Debrecen, Hungary, 24–25 May 2018; Debrecen University Press, Debrecen, Hungary, 2018:325–330.

Soudami, K., Maire, G. M., Dufrene, E., Francois, Ch., Delpierre, N., Ulrich, E., Cecchini, S., 2008: An evaluation of the onset of green-up in temperate deciduous broadleaf forests derived from Moderate Resolution Imaging Spectroradiometer (MODIS) data. Remote Sensing of Environment, 5:2643–2655.

Townshend, J. R. G., Huang, S. N., Kalluri, V., Defries, R. S., Liang, S., 2000: Beware of the per-pixel characterization of land cover. International Journal of Remote Sensing, 4:839–843.

Vicente-Serrano, S. M., Beguería, S., López-Moreno, J. I., 2010: A multiscalar drought index sensitive to global warming: The standardized precipitation evapotranspiration index. Journal of Climate, 23:1696–1718.

Vicente-Serrano, S. M., Camarero, J. J., Olano, J. M., Martín-Hernández, N., Peña-Gallardo, M., Tomás-Burguera, M. et al., 2016: Diverse relationships between forest growth and the Normalized Difference Vegetation Index at a global scale. Remote Sensing of Environment, 187:14–29.

Wigley, T. M. L., Briffa, K. R., Jones, P. D., 1984: On the average value of correlated time-series, with applications on Dendroclimatology and Hydrometeorology. Journal of Climate and Applied Meteorology, 23:201–213.

Wulder, M. A., Masek, J. G., Cohen, W. B., Loveland, T. R., Woodcock, C. E., 2012: Opening the archive: How free data has enabled the science and monitoring promise of Landsat. Remote Sensing of Environment, 122:2–10.